Using these values of Sakai and our γ-ray intensity ratio, we obtain

$$\alpha_K^{\text{expt}}(1029) = (1.36 \pm 0.52) \times 10^{-2}.$$

On the other hand, Schult *et al.*[7] report

$$I_e(1029)/I_e(661) > 3.2 \times 10^{-2}$$

and

$$\alpha_K(661) = (1.04) \pm 0.13) \times 10^{-2}.$$

These results then lead to a value

$$\alpha_K^{\text{expt}}(1029) \lesssim (0.68 \pm 0.27) \times 10^{-2}.$$

Since

$$\alpha_K^{\text{theor}}(E2,1029) \approx 0.42 \times 10^{-2}$$

and

$$\alpha_K^{\text{theor}}(M1,1029) \approx 1.08 \times 10^{-2},$$

the experimental conversion coefficient computed from Sakai's values would lead to a spin assignment of 1, whereas that obtained with the results of Schult *et al.* would yield a spin of 2.

The low-lying states of the even-even mercury isotopes are shown in Fig. 3. Although the Hg^{200} state at 1254 keV may be the one corresponding to the second 2^+ states in the other isotopes, it would appear that a spin assignment of 2 to the 1029-keV level would be more consistent with the systematic trend observed.[5] Furthermore, a spin-1 state at this position would be rather difficult to understand on the basis of the applicable theoretical models. Therefore, we would favor a spin/parity assignment of 2^+ to the 1029-keV level. However, an unequivocal assignment requires a resolution of the inconsistency in the 661-keV conversion coefficient measurements.

[7] O. W. B. Schult, W. Kaiser, W. Mampe, and T. V. Egildy (private communication).

ACKNOWLEDGMENTS

We are grateful to Professor Ben Mottelson for communicating Sakai's results to us, and to Fred. W. Loeser for his skillful operation of the isotope separator.

PHYSICAL REVIEW VOLUME 177, NUMBER 4 20 JANUARY 1969

Delayed Neutron Emission in the Decays of Short-Lived Separated Isotopes of Gaseous Fission Products*

W. L. Talbert, Jr., A. B. Tucker, and G. M. Day†

Institute for Atomic Research and Department of Physics, Iowa State University, Ames, Iowa 50010

(Received 27 June 1968)

Delayed-neutron activity of separated isotopes of krypton and xenon and their decay products has been studied. The TRISTAN on-line isotope separator system at the Ames Laboratory Research Reactor was used to provide sources of short-lived gaseous fission products of selected masses, through $A=93$ for krypton and $A=142$ for xenon. Total delayed-neutron yields for each mass were measured by a calibrated long counter, and the relative yields of the parent and daughter nuclei in an isobaric decay chain were determined by multiscaling the delayed-neutron activity and resolving the contributions for different half-lives. The precusors and delayed neutron emission probabilities determined in this study are Kr^{92}, 0.040%; Rb^{92}, 0.012%; Kr^{93}, 2.60%; Rb^{93}, 1.65%; Xe^{141}, 0.054%; Cs^{141}, 0.073%; Xe^{142}, 0.45%; and Cs^{142}, 0.27%. A comparison is made between predictions for delayed-neutron emission from several semiempirical mass formulas and observations for isotopes of As, Br, Kr, Rb, Sb, I, Xe, and Cs.

INTRODUCTION

THE first evidence for the emission of delayed neutrons in fission was reported by Roberts *et al.*[1] shortly after the discovery of nuclear fission. The mechanism for this process, originally proposed by Bohr and Wheeler,[2] is shown in Fig. 1. If the neutron separation energy of nuclide Y^A is less than the energy available in the β decay of its parent X^A, excited states of Y^A may be populated which can decay by neutron emission instead of electromagnetic transitions. In cases where delayed neutron emission is energetically possible, the selection rules for β decay will determine the neutron yield. The neutron activity has a half-life determined by the β decay of nuclide X^A, called the precursor.

The energetics of this process favor nuclides with a few neutrons beyond a filled shell, for which the neutron separation energy is relatively low. The known fission-product delayed-neutron precursors have this neutron structure.[3] Sufficiently heavy isotopes of most elements should exhibit delayed-neutron emission since, as neutrons are added to the nucleus, the trend is for β-decay energies to increase and neutron separation energies to decrease. The systematic variation of these energies with changes in Z and A for the nuclides with

* Work performed in the Ames Laboratory of the U.S. Atomic Energy Commission. Contribution No. 2353.

† Deceased.

[1] R. Roberts, R. C. Meyer, and P. Wang, Phys. Rev. **55**, 510 (1939).

[2] N. Bohr and J. A. Wheeler, Phys. Rev. **56**, 426 (1939).

[3] G. R. Keepin, *Physics of Nuclear Kinetics* (Addison-Wesley Publishing Co., Inc., Reading, Mass., 1965), Chap. 4.

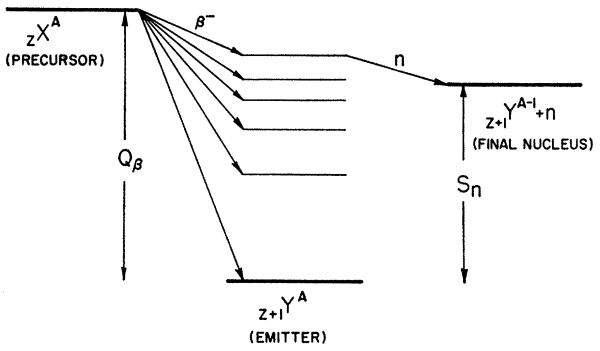

FIG. 1. Schematic representation of delayed-neutron emission.

known masses can be determined from the semi-empirical mass formulas. The identification of delayed-neutron emitters is one check of the accuracy of semi-empirical mass formulas when extrapolated from stable nuclides toward the neutron-rich isotopes of importance in nuclear fission and in nuclear synthesis by neutron capture.[4]

If the precursor nucleus X^A is a fission product, emission of a neutron will be delayed from the original fission event and the associated prompt neutrons by the time required for β decay. This delay, which ranges up to about 1 min for the known fission-product precursors, is crucial to the control of the chain-reaction process of nuclear reactors. Keepin[3] has compiled data on the total delayed-neutron activity of irradiated samples of fissionable materials, but knowledge of the individual precursors is incomplete.[5,6] Better precursor identification and more accurate yield data are needed to predict the kinetic behavior of the next generation of large power reactors.

In 1959, Perlow and Stehney[7] used fast chemical techniques for separating short-lived halogen fission products from solutions containing U^{235} and, on the basis of half-life, identified Br^{87-90} and $I^{137-139}$ as delayed-neutron precursors. They also examined the noble-gas fission products and found two precursors. A 6-sec Rb activity appeared to grow in from a 2-sec Kr parent.[8] Tomlinson[9] and del Marmol *et al.*[10,11] have shown that Sb^{135} and As^{85-87} may be delayed-neutron precursors. The present status of delayed-neutron emission and precursors has been summarized by Pappas and Tunaal,[12] Patzelt *et al.*,[13] and del Marmol.[14] In Ref. 14, the chemical approaches for precursor identification are reviewed and future possibilities for chemical procedures are compared to other techniques recently developed. Also, criteria for the detectability of delayed-neutron precursors have been presented by Tomlinson[15] which predict that, for the decays of noble-gas fission products and their daughters, the following isotopes should be observable delayed-neutron precursors: Kr^{92-95}, Rb^{92-97}, $Xe^{142-143}$, and $Cs^{142-146}$. The most recent chemical procedures have identified Kr^{93}, Rb^{93-94}, and Cs^{142} as delayed-neutron precursors.[16,17]

The recent development of on-line operation of electromagnetic isotope separators has made available continuous sources of very-short-lived selected nuclides. These techniques can be applied to the study of individual delayed-neutron precursors. The first such studies have been carried out by Amarel *et al.*,[18] who have reported delayed-neutron activity from separated isotopes of Rb^{93-96} and $Cs^{142-143}$. The results reported here are from a study of delayed-neutron activity from separated isotopes of the noble gases. Preliminary results of this work have been reported elsewhere.[19]

EXPERIMENTAL ARRANGEMENT

Delayed-neutron emission in the decays of selected isotopes of krypton and xenon and their daughters was studied using an isotope separator installed at the Ames Laboratory Research Reactor. Preliminary descriptions of the separator system, called TRISTAN, have been published earlier.[20,21] In its present configuration, shown in Fig. 2, TRISTAN is set up to provide gaseous fission products formed in the thermal fission of U^{235}. In principle, modifications to the sample chamber and transport line leading to the ion source of the isotope separator could enable the study of nongaseous activities produced either by fission or by neutron capture.

A 160-mg sample of U^{235}, in the form of UO_2 powder contained between disks of porous sintered stainless steel, is located near the core of the reactor in a region of high neutron flux (about 5×10^{12} n/cm^2 sec). The gas-

[4] P. A. Seeger, in Proceedings of the Third International Conference on Atomic Masses, Winnepeg, 1967, p. 85 (unpublished).
[5] S. Amiel, *Physics and Chemistry of Fission* (International Atomic Energy Agency, Vienna, 1965), Vol. 2, p. 171.
[6] G. Herrmann, J. Fiedler, G. Benedict, W. Eckhardt, G. Luthardt, P. Patzelt, and H. D. Schussler, in *Physics and Chemistry of Fission* (International Atomic Energy Agency, Vienna, 1965), Vol. 2, p. 197.
[7] G. J. Perlow and A. F. Stehney, Phys. Rev. **113**, 1269 (1959).
[8] A. F. Stehney and G. J. Perlow, Bull. Am. Phys. Soc. **6**, 62 (1961).
[9] L. Tomlinson, J. Inorg. Nucl. Chem. **28**, 287 (1966).
[10] P. del Marmol, M. Neve de Mevergnies, and A. Speecke, in *Physics and Chemistry of Fission* (International Atomic Energy Agency, Vienna, 1965), Vol. 2, p. 225.
[11] P. del Marmol and M. Néve de Mévergnies, J. Inorg. Nucl. Chem. **29**, 273 (1967).
[12] A. C. Pappas and T. Tunaal, Arkiv Fysik **36**, 445 (1967).
[13] P. Patzelt, H. D. Schussler, and G. Herrmann, Arkiv Fysik **36**, 453 (1967).
[14] P. del Marmol, in *Delayed Fission Neutrons* (International Atomic Energy Agency, Vienna, 1968), p. 75.
[15] L. Tomlinson, in *Delayed Fission Neutrons* (International Atomic Energy Agency, Vienna, 1968), p. 61.
[16] S. Amiel, J. Gilat, A. Notea, and E. Yellin, in *Delayed Fission Neutrons* (International Atomic Energy Agency, Vienna, 1968), p. 115.
[17] G. Herrmann, in *Delayed Fission Neutrons* (International Atomic Energy Agency, Vienna, 1968), p. 147.
[18] I. Amarel, R. Bernas, R. Foucher, J. Jastrzebski, A. Johnson, J. Teillac, and H. Gauvin, Phys. Letters **24B**, 402 (1967).
[19] G. M. Day, A. B. Tucker, and W. L. Talbert, Jr., in *Delayed Fission Neutrons* (International Atomic Energy Agency, Vienna, 1968), p. 103.
[20] D. Thomas and W. L. Talbert, Jr., Nucl. Instr. Methods **38**, 306 (1965).
[21] W. L. Talbert, Jr., and J. R. McConnell, Arkiv Fysik **36**, 99 (1967).

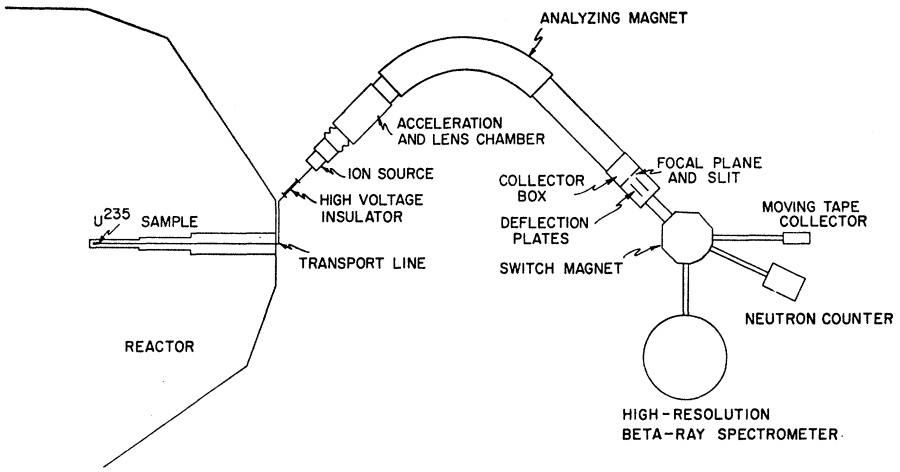

FIG. 2. Layout of TRISTAN on-line isotope separator system.

eous fission products are allowed to proceed from the sample through an ambient-temperature transport line of diameter 1.27 cm and length 5 m to the ion source of the separator by means of molecular flow. The ionized gas atoms are then separated by mass and the ion beam for the isotope of interest is allowed to pass through a slit at the focal plane of the separator into a switching magnet which steers the ion beam into desired detector arrangements. The switching magnet provides the benefit of physical removal of the activity of interest from the radiations resulting from neighboring mass activities (which are left behind in the collector box of the separator), and also provides a second stage of mass separation by which contamination in the selected ion beam is reduced. Furthermore, the ion beam can be brought to a secondary focus through deflection by the switch magnet. Since the whole process is continuous, the activity deposited upon a collection plate builds up to an equilibrium decay rate, and analysis may proceed without the periodic interruptions for sample replenishment which are characteristic of "batch" chemical separations. For half-life-determination purposes, the ion beam may be deflected before entry into the switching magnet, and the decay of the deposited activity may be followed. The short-lived activities made available by TRISTAN are $Kr^{85m,87-93}$ and $Xe^{135,137-142}$. Higher masses of each element are not provided in sufficient quantity for study due to the combination of small fission yield and short half-life. (The effective transit time from the U^{235} sample to the ion source of the separator is approximately 15 sec, resulting in appreciable decay during transit.)

The activity selected for study was deposited on a copper plate of dimensions 2.5×4 cm, etched from a printed circuit board. The ion current deposited on the plate (normally of the order of a fraction of a nanoampere) was monitored to maximize the deposit of activity. Most of the beam current is presumed to be due to some natural stable residue in the separator vacuum system; however, it is generally found that maximum current corresponds to maximum activity. A count rate meter connected to the detector system was monitored to give an independent indication of activity. The copper plate could be removed from the vacuum system for the purpose of counting long-lived activities.

The neutron detector consisted of five BF_3-filled proportional counters embedded in a block of paraffin. One face of the detector had a recessed port 15 cm deep so the counter could be slipped over the end of the beam tube, surrounding the point of beam deposit. Shielding from room neutrons was accomplished by a 5-cm layer of boron-loaded paraffin on all sides of the detector array, and the resulting background was within acceptable limits (about 0.8 counts/sec). The γ sensitivity of the neutron counter was checked with an intense beam of Kr^{90} activity and with a 120-μ Ci source of Co^{56}. No response was observed until a sample of D_2O was placed in the recessed port of the counter. With the D_2O present, a small but measurable response to the high-energy γ rays in the decay of Co^{56} was found and was attributed to photoneutrons from the D_2O. Hence, it was concluded that some neutron response could possibly result for photoneutrons from the natural deuterium content of the paraffin in the counter for activities containing intense high-energy γ radiation. In order to check the effect of high-energy γ rays which may be present in the decays of short-lived activities, and which may produce photoneutrons in the neutron counter, the neutron scaling of equilibrium activities was performed both with and without a sample of D_2O placed adjacent to the collector plate, at the end of the recessed port of the neutron counter. The 99.8% D_2O sample was sealed in a thin lucite cylindrical container 2 cm thick and 7 cm in diam.

After neutron emission at a selected mass had been established by scaling the equilibrium activities on the collector plate, the individual precursor nuclides along the decay chain were identified by multiscaling the decay of the neutron activity to determine precursor

TABLE I. Data from survey for neutron emission.

Mass	Neutron counts (normalized to 20-min counting period) Background	During collection	During collection with D_2O
	(beam off)	(beam on)	(beam on)
142	994	4731	4654
141	1028	8508	8001
140	1120	1180	...
93	1057	14 7220	14 3810
92	1057	13 428	13 410
91	1116	3167	43 242
Co^{56} (120 μCi)	1108	1100	1604

half-lives. The ion beam was collected at the neutron counter until the short-lived krypton (or xenon) and daughter activities were brought to equilibrium, then deflected and deposited in the collector box of the isotope separator, 2.5 m away, and the neutron-activity decay was observed. The control of the collection of activity, beam deflection, and multiscaling was provided by an automatic cycling device.

SURVEY OF AVAILABLE MASSES FOR NEUTRON EMISSION

To determine the presence of delayed neutrons from the activities available, equilibrium activities (beginning with Kr and Xe decays) for the mass numbers 91–93 and 140–142 were viewed by the neutron detector for periods of 20–60 min. Background was determined both before and after each counting period to determine the effects, if any, of long-lived activities which built up on the collector plate during neutron scaling. No such effects were observed.

Some typical data showing the results of these experiments are shown in Table I, which illustrate that delayed-neutron precursors exist in the decay chains of masses 92, 93, 141, and 142. The neutron activity at mass 91 evidently results from intense high-energy γ radiation present in the decay chain for this mass, as is shown by the large increase of neutron counting rate for the scaling period with D_2O inserted into the counter. It was not feasible to determine if photoneutron production by krypton or rubidium γ rays accounted for all of the observed neutron activity; however, delayed-neutron emission probability in this decay chain does not exceed 1% of that for mass 92. This upper limit is determined from the neutron counting rate and krypton activity ratios for masses 91 and 92. The apparent absence of any photoneutron production for the other mass chains implies that the emission of delayed neutrons was sufficiently intense for these mass numbers to mask any photoneutrons that may have been produced in the presence of deuterium. It should be noted, however, that the activity at mass 91 was very intense and that high-energy γ rays constitute a significant fraction of this activity, whereas high-energy γ rays are emitted in low abundance at the other masses, and it is possible that only for the case of mass 91 was sufficient high-energy γ-ray intensity present to produce detectable numbers of photoneutrons.

DETERMINATION OF NEUTRON BRANCHING FOR DECAY CHAINS

If delayed-neutron emission is present in the short-lived activities of an isobaric decay chain, the long-lived decay products present in the sample should exhibit traces of activities from the next lowest mass number. Examination of the long-lived γ spectra for all the collection plates revealed such activities for the initial experiments in this investigation. In fact, for the Kr decay chains, the presence of lower-mass activities was marked for the decay chains identified with delayed-neutron emission. Such activities also appeared, however, in the long-lived activities of decay chains not associated with delayed-neutron emission, e.g., $A=88$, indicating that these activities arose at least partly from cross contamination in the isotope separation rather than from delayed-neutron emission alone.

Closer examination of this cross contamination showed that nearly all of it was due to the deposition of beams of $(KrH)^+$ along with elemental $(Kr)^+$ beams. The formation of $(KrH)^+$ apparently resulted from ion-molecule reactions in the ion source and, for the short-lived Kr activities under study, appeared to be enhanced greatly over the values reported earlier for cross-contamination studies using Kr^{85} activity.[22] This enhancement probably results from the combined effects of fission yield and half-life differences between neighboring short-lived Kr isotopes, since the heavier mass not only has a smaller fission yield, but also will decay more while in transit to the ion source; both effects act to significantly enhance the lower-mass activity in the separator.

Various attempts to decrease the KrH contamination were made, but the only effective means of eliminating this contamination was to deposit doubly charged beams. Since this procedure resulted in a decrease in the available activity by a factor of 5–10, another approach to the operation of the isotope separator was made. The ion source in use was constructed largely of graphite which, when heated, outgassed continually during operation. A new ion source was developed which was of all-metal construction. This ion source did not outgas and, when used, the separator beam was found to be dramatically improved with respect to KrH contamination.

Because of the difficulties associated with cross contamination in the isotope separator, it was decided not

[22] J. Uhler, Arkiv Fysik **24**, 329 (1963).

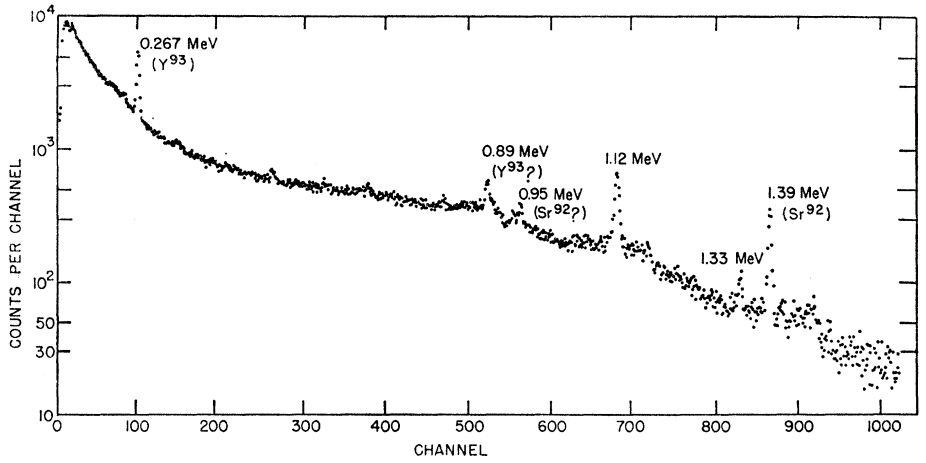

FIG. 3. γ-ray spectrum from long-lived activities for mass-93 collection.

to depend entirely upon the examination of long-lived activities for the determination of total decay chain neutron-emission probability. For the masses 92, 93, 141, and 142, a technique combining γ and neutron counting was used to determine the total neutron yields for these decay chains. Since the neutron-counting rate for mass 93 was the largest of those observed, it was presumed that this decay chain would be the most favorable to determine absolute branching from a measurement of the relative amount of long-lived mass-92 activity which grows into the sample as a result of delayed-neutron emission. A high-resolution Ge(Li) detector was used to measure the cross contamination during collection of a Kr^{93} ion beam. The resolution of this detector system (about 2.5 keV for 1.33-MeV γ rays) was sufficient to allow reliable observation of low-intensity γ rays resulting from the presence of small amounts of activities of Kr^{92}. It was found that no Kr^{92} γ rays were present in the Kr^{93} spectrum to within 0.1% of the Kr^{93} activity. Hence, $Kr^{92}H$ could not account for a significant fraction of the long-lived mass-92 activity, which grows into the sample as a result of delayed-neutron emission in mass-93 decays. Thus, for the case of mass 93, a cross check could be made on the technique used for the determination of neutron-emission probability for the decay chain.

The technique to determine neutron-emission probability for an isobaric decay chain involved collection of activity for the mass of interest on a clean collection plate, with simultaneous scaling of neutron activity from the deposition. At the end of the collection period, the collection plate was removed and the long-lived γ activities observed in order to determine the total number of atoms collected. The observation of long-lived γ activities was carried out in a nearby (low-background) laboratory, using a Ge(Li) detector which had a larger detection efficiency, but somewhat poorer resolution, than the detector mentioned previously. In addition, for mass 93, the ratio of long-lived activities of Sr^{92} and Y^{93}, shown in the spectrum in Fig. 3, was used to estimate the absolute neutron-emission probability, and from the neutron-scaling results an approximate determination was made for the efficiency of the neutron counter. This method gave a neutron-counter efficiency of $(2.49\pm0.64)\%$. An independent measurement of the neutron-counter efficiency was made using neutrons from a PuBe source, which has a calibrated neutron-emission rate of $(7.46\pm0.75)\times10^4$ n/sec, and gave a neutron-counter efficiency of $(2.61\pm0.26)\%$. For the decay chain of mass 93, the cross contamination was not a serious problem, as indicted in the very good agreement between these two methods for determination of the neutron-counter efficiency. The presence of a large amount of cross contamination would have resulted in a neutron-counter efficiency which would have been considerably lower than that determined using the calibrated neutron source.

For the other decay chains, the cross contamination was still a serious interference in the absolute determinations of neutron-emission probabilities (even though it was considerably reduced from the initial experiments) due to the relatively small neutron-emission probabilities present in these decay chains. For this reason, the long-lived activities of masses A and A-1 present in the sample were not used to determine the neutron-emission probabilities for decay chains other than for mass 93. The neutron-counter efficiency as determined by the neutron source was used along with the long-lived activity of mass A to determine the neutron-emission probability for each of the other decay chains. It was assumed that the neutron-counter efficiency was invariant with respect to the details of the energy spectra for neutrons emitted during the decays of the different isobaric chains.

A close inspection of the spectrum shown in Fig. 3 reveals several γ-ray peaks that have not been identified. Of those identified, the 0.267-MeV peak from the decay of Y^{93} and the 1.39-MeV peak from the decay of Sr^{92} both were observed to decay with half-life appropriate for their assignments. On the basis of similarities in half-life, the 0.89-MeV peak appears to be associated with Y^{93} decay, and the 0.95-MeV peak with the decay

TABLE II. Data for total neutron branching.

Mass	Collection time (h)	Neutron counts	Activity of interest (long-lived)	Total No. of atoms deposited	Total neutron branching (%)
142	1.5	11 704±139	0.65-MeV transition in La^{142} (92 m), (50±5)% of decays	$(6.22\pm0.63)\times10^{7}$	0.72±0.10
141	1.5	22 353±173	1.36-MeV transition in La^{141} (3.9 h), (2.0±0.2)% of decays	$(6.79\pm0.72)\times10^{8}$	0.127±0.018
93	1.0	383 353±625	0.267-MeV transition in Y^{93} (10.2 h), (6.4±1.0)% of decays	$(3.58\pm0.56)\times10^{8}$	4.21±0.80
92	1.083	23 479±174	1.37-MeV transition in Sr^{92} (2.71 h), (90±10)% of decays	$(1.74\pm0.20)\times10^{9}$	0.052±0.008

of Sr^{92}. However, the peaks at 1.12 and 1.33 MeV do not follow either of the activities of interest. It is unimportant in this study to determine the origins of these γ rays, but the fact that these peaks are rather prominent and yet have not been previously correlated to known γ-ray transitions in this mass region is testimony to the uncertainties existing in these decay schemes, and serves to illustrate the basic limitations of the technique used in this work, namely, to depend upon previously determined decay intensities for the γ rays involved.

The long-lived activities used to determine the number of deposited atoms, along with the fractions of decays represented by the transitions monitored, were mass 92, 1.37-MeV transition in the decay of 2.71-h Sr^{92} [(90±10)%][23]; mass 93, 0.267-MeV transition in 10.2-h Y^{93} [(6.4±1.0)%][24]; mass 141, 1.36-MeV transition in 3.9-h La^{141} [(2.0±0.2)%][25]; mass 142, 0.65-MeV transition in 92-min La^{142} [(50±10)%].[26] As can be noted, the transition probabilities are only approximately known, and the resulting uncertainties essentially limit the precision of the delayed neutron-yield measurements reported in this work.

The data used to determine the neutron branching are presented in Table II. These data consist of the period of collection and neutron scaling, the neutron counts obtained, and the long-lived activity used to measure the number of atoms deposited. By use of standard decay equations, in which neutron-emission branching was assumed to be present for both Kr(Xe) and Rb(Cs) decays, the number of atoms deposited during collection was determined from these data. Then, using the neutron-counter efficiency measured earlier, the neutron-scaling results yielded the percentage of the decays of the deposited atoms resulting in neutron emission. Thus, the values of the total neutron-emission probabilities for the first two members of the decay chains are shown in Table II. The very small total emission probability for the mass-92 decay chain illustrates the sensitivity possible when separated isotopes are available, and the moderately large branching shown for the mass-142 decay chain, despite the low neutron-counting rate, illustrates the limitation in activity at high masses using TRISTAN. The errors shown in the total neutron-emission probabilities result primarily from the uncertainties in γ-detector efficiency (2%), neutron-counter efficiency (10%), γ-ray intensities in the existing decay schemes for the long-lived daughters (10–16%), and statistics of counting (relatively small), all statistically combined.

DETERMINATION OF RELATIVE NEUTRON YIELDS AMONG ISOBARS

Neutron multiscaling was used to determine the relative fractions of neutron activities observed in the decays of Kr^{92}, Kr^{93}, Xe^{141}, Xe^{142}, and their daughters. Also, the photoneutrons associated with the decay of mass-91 activity when D_2O was inserted into the neutron counter were multiscaled to determine if both Kr^{91} and Rb^{91} emit energetic γ rays in their decays.

The conditions for neutron multiscaling and for the analysis of the resulting neutron-decay curves are shown in Table III. The dwell time per channel of the analyzer,

TABLE III. Neutron multiscaling conditions.

Mass	Analyzer dwell time [sec/(No. of channels)]	Collect time (sec)	Delay time (sec)	Total count time per channel (sec)
142	0.1/(256)	25	1	50
141	0.4/(512)	180	2	25
93	0.1/(256)	39	1	40
92	0.1/(512)	45	1	40
91+D_2O	1.0/(512)	600	4	11

[23] R. L. Heath, Phys. Rev. **105**, 1011 (1957).
[24] J. D. Knight, D. C. Hoffman, B. J. Dropesky, and D. L. Frasco, J. Inorg. Nucl. Chem. **10**, 183 (1959).
[25] R. P. Schuman, E. H. Turk, and R. L. Heath, Phys. Rev. **115**, 185 (1959).
[26] W. V. Prestwich and T. J. Kennett, Phys. Rev. **134**, B485 (1964).

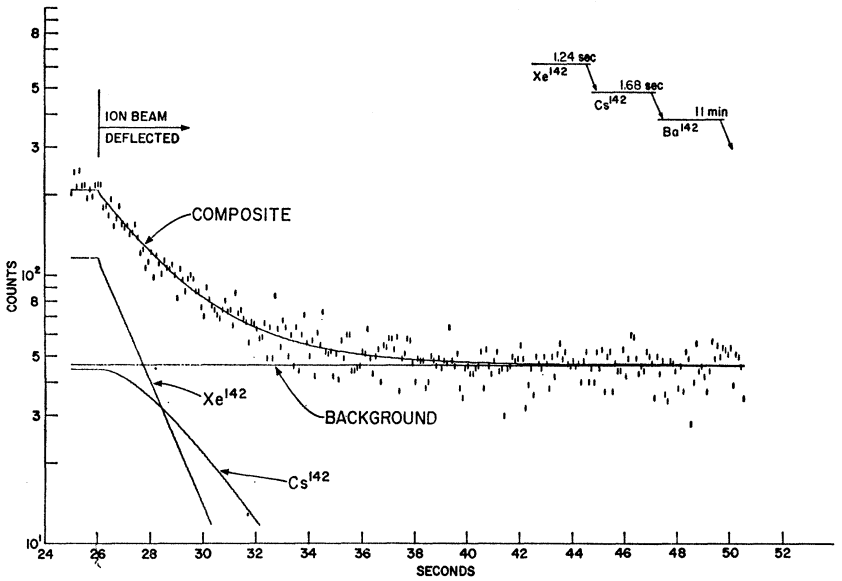

FIG. 4. Decay of neutron activity for mass 142.

the total number of channels used in scaling, the collect time, and delay time (which was a time introduced after the start of multiscaling and before deflection of the ion beam in order to determine in the decay curve the time at which decay begins) are indicated, along with the total counting time per channel (dwell time multiplied by the number of cycles). The half-lives used in the spectrum stripping analysis were determined by γ multiscaling in a separate experiment which will be reported elsewhere, and represent the best directly determined half-lives available.

The decay curves resulting from neutron multiscaling are shown in Figs. 4–8. In these figures, the time axis includes the time of collection, and the neutron activity is shown during multiscaling. Since it is evident in each decay curve that there are two components present, a computer program was developed to determine the relative neutron-emission probabilities for the two precursors in each decay chain. The relative probability was varied to obtain a least-squares fit to the data. The separate contributions for the two precursors, background, and the composite curve are shown for each case. Note that the daughter decays are not simple exponentials, due to the continued production of daughter activity during the decay of the parent.

The results of the computer determination of relative emission probability, combined with the total neutron-emission probability, can be used to assign the percent-

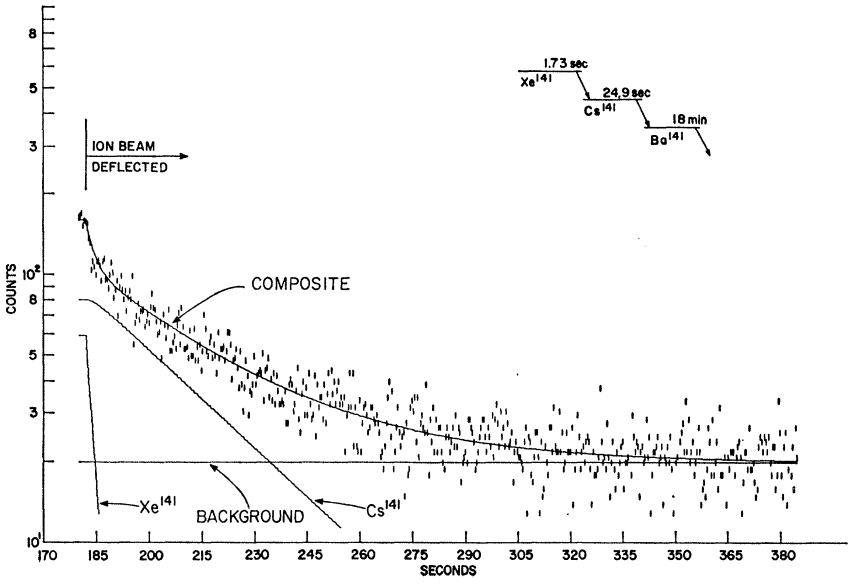

FIG. 5. Decay of neutron activity for mass 141.

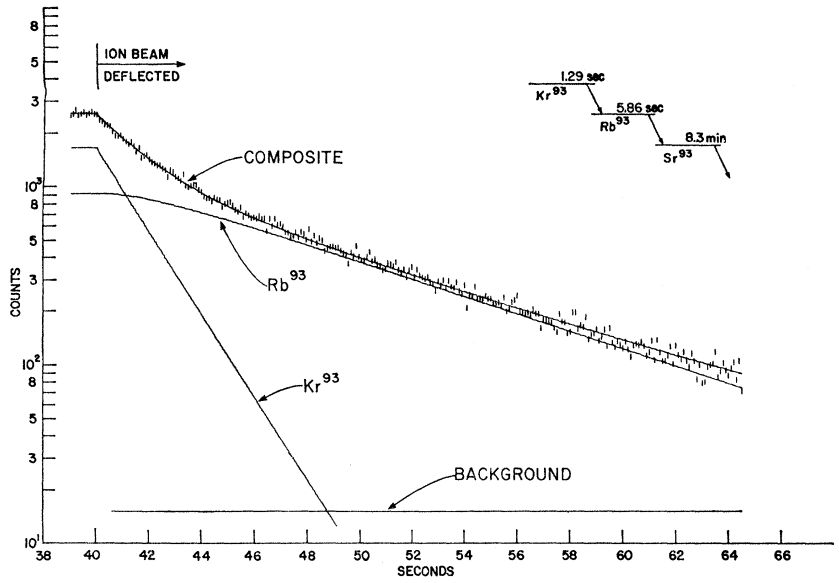

FIG. 6. Decay of neutron activity for mass 93.

age of neutron branching for individual precursor decays, and the results for the decay chains studied in this work are shown in Table IV. For the decays of Rb^{91} and Kr^{91}, the yields shown are relative photoneutron production probabilities. As a result of photoneutron multiscaling at mass 91, the decays of both Kr^{91} and Rb^{91} should exhibit rather intense high-energy γ-ray transitions. It will be interesting to compare this conclusion to the actual nature of the decay spectra, now under study.

Since neutron emission in the decay of a nucleus reduces the number of daughters in the isobaric decay chains, the total decay emission probability at each mass, listed in Table II, is related to the emission probabilities of the two individual precursors in the decay chain, listed in Table IV, by the relation

$$P_{\text{tot}}=P_1+(1-P_1)P_2.$$

The errors shown in Table IV are the statistical combination of uncertainties in the total branching and in the relative branching as determined by the computer fit to the decay data.

DISCUSSION

The total delayed-neutron yield associated with the fission of U^{235} by thermal neutrons is 0.0158 ± 0.0005 neutrons per fission.[3] The contributions of the precursors

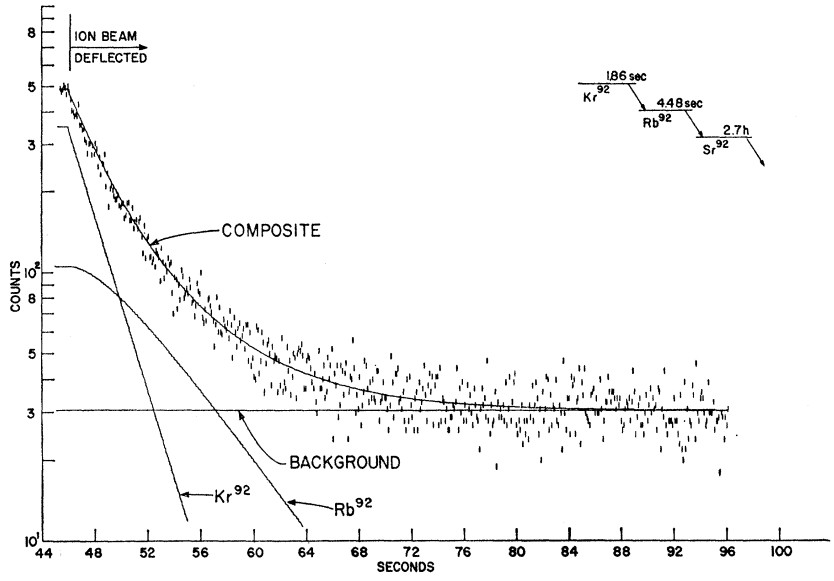

FIG. 7. Decay of neutron activity for mass 92.

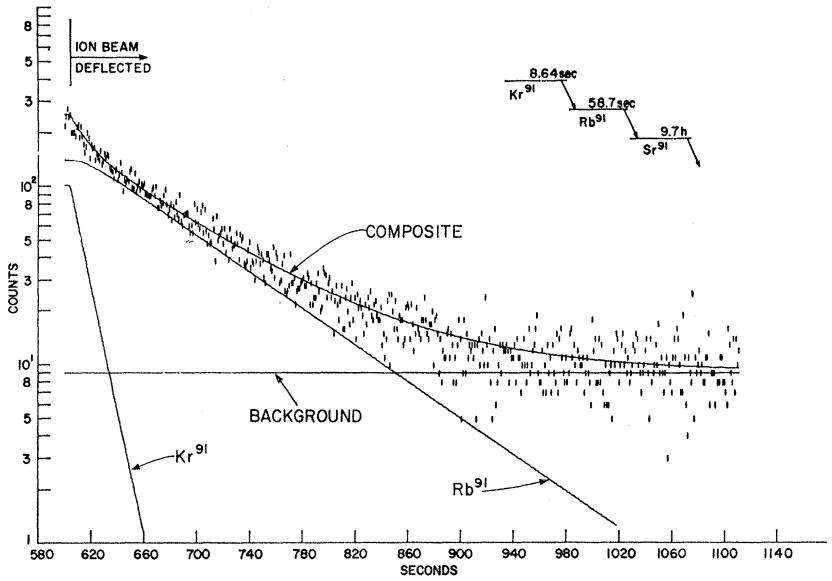

FIG. 8. Decay of neutron activity for mass 91+D_2O.

identified in this work, calculated from the neutron-emission probabilities listed in Table IV, are shown in Table V. The precursor yields given are the total number of precursor nuclei produced per 100 fissions, the sum of the direct fission yield for an individual precursor nucleus and the contribution from the β decay of fission-product isobars. These yields were furnished by Wahl[27] and represent the combination of total chain yields from data mainly due to Tomlinson and coworkers[28,29] and best estimates of fractional yields from various radiochemical and systematic determinations. The noble-gas nuclei studied in this work contribute very little to the total delayed-neutron yield (about 1%), whereas the alkali nuclei studied contribute a substantial amount (about 5%). The heavier short-lived isotopes of the elements studied in this work can be expected to have larger delayed-neutron-emission probabilities, but in most cases their fission yield is so small that they are not an important source of delayed neutrons in the thermal fission of U^{235}. The neutrons emitted during the decay of Rb^{93} account for about 20% of the $T_{1/2}\cong$6-sec delayed-neutron group, which yields approximately $0.003n/f$.[3] The values for the neutron-emission probabilities for Kr^{93} and Rb^{93} are lower than those reported by Amiel *et al.*[16] and more in agreement with those reported by Herrmann.[17] The relative emission probabilities found in this study agree well with those of Amiel *et al.*, and the disagreement in the absolute values is not easily explained. It is possible that the two-step calibration technique used by Amiel *et al.* may be subject to rather large error due to the use of an NaI(Tl) detector to determine the yields of Kr^{91} and Kr^{92} in the same sample. The γ spectra of these nuclei as observed in this laboratory using Ge(Li) detectors show considerable overlap and they may thus be difficult to resolve reliably using detectors with poorer resolution.

In Table VI the experimentally observed onset of

TABLE IV. Delayed-neutron-emission probabilities.

Precursor nucleus	Half-life (sec)	Neutron emission (%)	Total isobar emission (%)
Xe^{142}	1.24±0.02	0.45±0.08	0.72±0.10
Cs^{142}	1.68±0.02	0.27±0.07	
Xe^{141}	1.73±0.01	0.054±0.009	0.127±0.018
Cs^{141}	24.9±0.2	0.073±0.011	
Kr^{93}	1.29±0.01	2.60±0.50	4.21±0.80
Rb^{93}	5.86±0.13	1.65±0.30	
Kr^{92}	1.86±0.01	0.040±0.007	0.052±0.008
Rb^{92}	4.48±0.02	0.012±0.004	
Kr^{91}+D_2O	8.64±0.04	42±3	100 (relative only)
Rb^{91}+D_2O	58.7±0.1	58±3	

[27] A. C. Wahl (private communication).
[28] J. A. Petruska, H. G. Thode, and R. H. Tomlinson, Can. J. Phys. **33**, 693 (1955).
[29] H. Farrar and R. H. Tomlinson, Nucl. Phys. **34**, 367 (1962).

TABLE V. Delayed-neutron yields in thermal fission of U^{235}.

Precursor nucleus	Half-life (sec)	Cumulative precursor yield Y (%)[a]	Delayed-neutron-emission probability P_n (%)	Absolute yield ($10^{-4}n/f$)	Contribution to total delayed neutron yield (%)[b]
Xe^{142}	1.24	0.312	0.45	0.14	0.08
Cs^{142}	1.68	3.11	0.27	0.84	0.53
Xe^{141}	1.73	1.14	0.054	0.06	0.04
Cs^{141}	24.9	4.61	0.073	0.34	0.21
Kr^{93}	1.29	0.531	2.60	1.38	0.87
Rb^{93}	5.86	4.00	1.65	6.60	4.18
Kr^{92}	1.86	1.69	0.040	0.07	0.04
Rb^{92}	4.48	5.19	0.012	0.06	0.04

[a] From Ref. 27. [b] The value of the total delayed-neutron yield was $0.0158n/f$, as reported by Keepin in Ref. 3.

delayed-neutron emission with increasing neutron number is compared with the thresholds predicted by eight recently published mass formulas[30–38] for isotopes of As, Br, Kr, Rb, Sb, I, Xe, and Cs. It is expected that all isotopes for elements in this table which are heavier than those listed should be delayed-neutron precursors. This comparison is a qualitative test of the accuracy with which the binding-energy systematics of the measured masses can be extended to heavy isotopes several mass units from stability. A similar comparison of 12 mass formulas on the basis of how well they fit the observed nuclidic abundances in the solar system assuming the r process of nuclear synthesis has been published by Seeger.[39]

β-decay branching probabilities can result in delayed-neutron emission, which is so improbable as to be undetectable even though there is enough energy available. Therefore, the absence of observed neutron activity in nuclides for which it is predicted by a particular mass formula to be energetically possible does not mean that the mass formula is incorrect. As^{84}, which all but one formula predict to be a delayed-neutron precursor, may be an example of such a case. The agreement between the formulas and the data is generally good. Of the eight formulas compared, that of Seeger and Perisho best fits the experimental data. (This formula also fits reasonably well the known masses near $A=90$ and $A=140$.) Measurements of β-decay energies of Kr^{90-93}, $Xe^{139-142}$, and their decay products, which have been initiated at this laboratory, will provide a quantitative test of the accuracy of the mass formulas in this region.

Energy spectra of the delayed neutrons would be significant data for nuclear energy level structure, checking the mass formulas, and reactor technology. However, the efficiency of neutron spectrometers capable of resolving the neutron energy groups expected[40] is so small that energy measurements at this laboratory have been postponed until the present system can be modified to make stronger sources available.

CONCLUSIONS

In the study of the decays of short-lived noble-gas nuclei and their daughters, eight delayed-neutron precursors have been identified: Kr^{92}, Kr^{93}, Xe^{141}, Xe^{142}, Rb^{92}, Rb^{93}, Cs^{141}, and Cs^{142}. Recent experiments by Amiel *et al.*[16] using chemical techniques to study unseparated krypton isotopes, and by Amarel *et al.*[18] using an on-line mass spectrometer to study separated isotopes of Rb and Cs produced in fission induced by high-energy protons, corroborate the assignment in this work of neutron activity for the decays of Kr^{93}, Rb^{93}, and Cs^{142}, but not for Kr^{92}, Rb^{92}, Xe^{141}, Cs^{141}, and Xe^{142}, presumably because of the small delayed-neutron-

[30] P. A. Seeger and R. C. Perisho, U.S. Atomic Energy Commission Report No. LA-3751, 1967 (unpublished).
[31] W. D. Myers and W. J. Swiatecki, Nucl. Phys. **81**, 1 (1966). Also W. D. Myers and W. J. Swiatecki, U.S. Atomic Energy Commission Report No. UCRL-11980, 1965 (unpublished).
[32] J. Wing and P. Fong, Phys. Rev. **136**, B923 (1964); also J. Wing and J. D. Varley, U.S. Atomic Energy Commission Report No. ANL-6886, 1964 (unpublished).
[33] M. Hillman, U.S. Atomic Energy Commission Report No. BNL-846, 1964 (unpublished).
[34] A. G. W. Cameron and R. M. Elkin, Can. J. Phys. **43**, 1288 (1965) (exponential form only).
[35] H. Kümmel and A. H. Wapstra, Nucl. Phys. **81**, 129 (1966) (formula III only).
[36] N. Zeldes, A. Grill, and A. Simievic, Kgl. Danske Videnskab. Selskab, Mat.-Fys. Medd. **36**, No. 5 (1967).
[37] G. T. Garvey and I. Kelson (private communication to J. Wing).
[38] The predictions of Refs. 32–37 were calculated by J. Wing (private communication); the values of Seeger and Perisho and of Myers and Swiatecki were taken from their published tables (Refs. 30 and 31).
[39] P. A. Seeger, Arkiv Fysik **36**, 495 (1967).
[40] T. Jahnsen, A. C. Pappas, and T. Tunaal, in *Delayed Fission Neutrons* (International Atomic Energy Agency, Vienna, 1968), p. 35.

TABLE VI. Delayed-neutron-emission prediction by mass formulas.

Precursor	Emission observed (Observed emission probability in %)[a]	β-decay energy of precursor nucleus (MeV) Neutron separation energy of emitter nucleus (MeV) Prediction of neutron emission Formula a	Formula b	Formula c	Formula d	Formula e	Formula f	Formula g	Formula h
$_{33}As^{84}$	No	9.82 8.75 Yes	10.50 8.84 Yes	8.61 8.95 No	9.00 8.55 Yes	10.59 8.62 Yes	10.61 9.25 Yes	9.91 8.94 Yes	9.21 9.06 Yes
$_{33}As^{85}$	Yes (11±3)	8.66 4.51 Yes	8.84 3.70 Yes	6.54 5.74 Yes	7.40 4.98 Yes	9.79 4.58 Yes	8.94 3.64 Yes	9.16 4.48 Yes	8.27 4.10 Yes
$_{35}Br^{86}$	No	7.36 9.65 No	7.88 9.66 No	5.57 10.06 No	6.75 9.36 No	7.40 9.64 No	7.88 10.17 No	7.40 9.97 No	6.84 10.18 No
$_{35}Br^{87}$	Yes (2.9±0.6)	6.29 5.47 Yes	6.25 4.74 Yes	4.99 4.34 Yes	5.20 5.80 No	6.66 5.56 Yes	6.24 4.72 Yes	6.64 5.41 Yes	5.90 5.46 Yes
$_{35}Br^{88}$	Yes (5.9±1.6)	9.06 7.00 Yes	9.32 6.86 Yes	8.94 8.92 Yes	8.45 7.73 Yes	9.11 6.78 Yes	9.39 7.21 Yes	8.96 7.00 Yes	8.19 7.14 Yes
$_{36}Kr^{91}$	No	6.35 6.99 No	6.84 7.12 No	6.03 7.58 No	6.17 7.40 No	7.51 6.73 Yes	7.15 6.87 Yes	6.73 6.66 Yes	5.68 6.86 No
$_{36}Kr^{92}$	Yes (0.040±0.007)	4.71 4.48 Yes	5.21 4.73 Yes	5.08 3.86 Yes	4.30 4.78 No	5.62 4.22 Yes	5.50 4.59 Yes	5.53 4.99 Yes	4.53 5.06 No
$_{36}Kr^{93}$	Yes (2.60±0.50)	7.89 6.56 Yes	8.19 6.84 Yes	7.93 6.22 Yes	7.20 7.02 Yes	8.88 6.54 Yes	8.53 6.40 Yes	8.17 6.25 Yes	7.36 6.30 Yes
$_{37}Rb^{91}$	No	5.30 5.60 No	4.97 5.31 No	4.20 6.00 No	4.53 5.65 No	6.07 5.76 Yes	5.18 5.23 No	5.49 5.66 No	4.70 5.93 No
$_{37}Rb^{92}$	Yes (0.012±0.004)	8.24 7.43 Yes	7.85 7.61 Yes	7.51 7.17 Yes	7.52 7.76 No	9.06 7.20 Yes	8.25 7.66 Yes	7.99 7.48 Yes	6.99 7.35 No
$_{37}Rb^{93}$	Yes (1.65±0.30)	6.61 4.92 Yes	6.22 5.21 Yes	6.13 4.83 Yes	5.65 5.15 Yes	7.19 4.67 Yes	6.60 4.74 Yes	6.79 5.05 Yes	5.84 5.14 Yes
$_{51}Sb^{133}$	No	4.57 6.10 No	4.95 5.56 No	5.24 5.48 No	5.08 5.54 No	5.36 5.90 No	4.67 5.64 No	4.56 5.81 No	3.99 5.81 No
$_{51}Sb^{134}$	Yes (~0.1)	8.37 7.45 Yes	9.38 7.30 Yes	7.58 7.22 Yes	8.52 7.03 Yes	9.45 7.24 Yes	9.60 7.74 Yes	8.85 7.75 Yes	7.91 7.35 Yes
$_{51}Sb^{135}$	Yes (~4)	7.67 3.91 Yes	7.96 3.22 Yes	6.19 5.24 Yes	7.64 3.87 Yes	8.03 3.45 Yes	8.35 3.02 Yes	7.57 3.49 Yes	6.74 3.86 Yes
$_{53}I^{136}$	No	6.57 8.08 No	7.49 7.97 No	6.33 7.84 No	6.84 7.58 No	7.55 7.86 No	7.42 8.32 No	7.17 8.27 No	6.18 7.94 No
$_{53}I^{137}$	Yes (3.0±0.6)	5.87 4.57 Yes	6.08 3.91 Yes	4.19 6.06 No	5.97 4.43 Yes	6.16 4.05 Yes	6.16 3.87 Yes	5.88 4.17 Yes	5.01 4.46 Yes
$_{53}I^{138}$	Yes (2.1±0.5)	7.59 5.61 Yes	8.44 5.64 Yes	7.44 6.46 Yes	8.07 5.56 Yes	8.05 5.73 Yes	8.75 5.73 Yes	8.28 5.78 Yes	7.02 5.86 Yes
$_{54}Xe^{140}$	No	4.04 4.52 No	4.26 3.97 Yes	3.39 3.54 No	3.46 4.01 No	3.67 4.43 No	4.32 3.92 Yes	3.44 4.05 No	2.78 4.21 No

TABLE VI (*Continued*)

Precursor	Emission observed	β-decay energy of precursor nucleus (MeV) Neutron separation energy of emitter nucleus (MeV) Prediction of neutron emission							
	(Observed emission probability in %)[a]	Formula a	Formula b	Formula c	Formula d	Formula e	Formula f	Formula g	Formula h
$_{54}Xe^{141}$	Yes	5.87	6.59	6.17	5.58	5.98	6.74	5.73	5.06
	(0.054±0.009)	5.65	5.69	6.94	6.19	5.95	5.50	5.83	5.79
		Yes	Yes	No	No	Yes	Yes	No	No
$_{54}Xe^{142}$	Yes	4.96	5.20	4.71	3.92	4.74	5.21	4.20	3.56
	(0.45±0.08)	4.14	3.69	2.27	4.35	3.93	3.66	3.88	3.93
		Yes	Yes	Yes	No	Yes	Yes	Yes	No
$_{55}Cs^{140}$	No	5.88	6.59	6.77	6.58	6.64	6.71	6.60	5.33
		6.24	6.31	6.96	6.10	6.34	6.49	6.45	6.22
		No	Yes	No	Yes	Yes	Yes	Yes	No
$_{55}Cs^{141}$	Yes	5.08	5.21	4.68	4.68	5.42	5.28	5.13	4.19
	(0.073±0.011)	4.84	4.30	4.85	4.28	4.73	4.07	4.37	4.65
		Yes	Yes	No	Yes	Yes	Yes	Yes	No
$_{55}Cs^{142}$	Yes	6.89	7.53	8.12	6.78	7.74	7.68	7.40	6.46
	(0.27±0.07)	5.95	6.01	5.71	6.45	6.25	6.07	6.15	6.20
		Yes	Yes	Yes	Yes	Yes	Yes	Yes	Yes

[a] Observed delayed-neutron-emission probabilities from Refs. 15 and 17, and this work. Key to mass formulas: a, Seeger and Perisho (Ref. 30); b, Myers and Swiatecki (Ref. 31); c, Hillman (Ref. 33); d, Wing and Fong (Ref. 32); e, Cameron and Elkin (Ref. 34); f, Kümmel and Wapstra (Ref. 35); g, Zeldes, Grill, and Simievic (Ref. 36); h, Garvey and Kelson (Ref. 37).

emission probabilities for these nuclei (see Table IV). According to the limit of detectability for delayed-neutron activity suggested by Tomlinson[15] of 0.1 for the products of neutron-emission probability and yield (both expressed in percent), it is not unexpected that the precursors Xe^{141}, Kr^{92}, and Rb^{92} had not been identified in earlier work. What is surprising, perhaps, is that using an on-line isotope separator has lowered the limit of detectability, even though the isotope-separator system is inefficient in terms of the fraction of the gross activity input which is made available for study.

The results of this experimental study provide the first definite evidence that Kr^{92}, Rb^{92}, Xe^{141}, and Xe^{142} are delayed-neutron precursors. The assignment of delayed-neutron-emission probabilities has been made using a direct procedure made feasible by the fact that the samples studied were pure isobars. The combined neutron yield of the eight precursors studied in this work, calculated from the measured neutron-emission probabilities, is about 6% of the total delayed-neutron yield in the fission of U^{235} by thermal neutrons.

The predictions of eight recent semiempirical mass formulas of the lowest mass number for which delayed-neutron emission is energetically possible for fission product elements having isotopes known to be precursors are in reasonably good agreement with the observed onset of delayed-neutron emission with increasing neutron number.

ACKNOWLEDGMENTS

This work would not have been possible without the dependable and invaluable aid given by J. R. McConnell and J. J. Eitter in the operation of the isotope separator. We are also indebted to C. H. Weber of the Ames Laboratory Research Reactor Instrumentation Group for assistance in the electronics required for the experiments, and to the Reactor Operations Staff for their patience with our demands upon reactor scheduling. We especially appreciate the tables of fission yields provided by Professor A. C. Wahl of Washington University of Saint Louis, and the calculations on mass-formula predictions for β-decay energies and neutron separation energies which were kindly provided by Dr. J. Wing of the Argonne National Laboratory. We also wish to express our appreciation to Dr. A. F. Stehney of the Argonne National Laboratory for his interest in this work and for many helpful discussions. The fine experimental ground work performed by one of us (GMD) prior to his untimely death has been invaluable in the continuation of this investigation.